

FREQUENCY ANALYSIS OF THE TYPICAL IMPULSE VOLTAGE AND CURRENT WAVESHAPES OF TEST GENERATORS

Vesna Javor

Department of Power Engineering, Faculty of Electronic Engineering, University of Niš,
Serbia

Abstract. *Frequency analysis of the impulse waveshapes of generators which are commonly used for testing of the equipment in high-voltage engineering is presented in this paper. Some of the typical impulse waveshapes, such as 1.2/50 $\mu\text{s}/\mu\text{s}$, 10/350 $\mu\text{s}/\mu\text{s}$, 10/700 $\mu\text{s}/\mu\text{s}$, 10/1000 $\mu\text{s}/\mu\text{s}$, and 250/2500 $\mu\text{s}/\mu\text{s}$, are approximated by the Double-exponential function (DEXP) and by the terms of Multi-peaked analytically extended function (MP-AEF). Experimental set ups for impulse signal generation are based on the desired outputs as given in the IEC 60060-1 Standard. Dumped oscillations are characteristic of the standardized 8/20 $\mu\text{s}/\mu\text{s}$ waveshape. The positive part of the normalized Sinc function with dumped oscillations is also approximated by MP-AEF terms. The corresponding frequency spectra of these aperiodic signals are obtained analytically by using Piecewise Fourier transform (PWFT). This paper presents the procedure to obtain Fourier transforms of the functions with multiple and sharp peaks typical for the impulse current and voltage test generators' waveshapes.*

Key words: *Fourier transform, high-voltage technique, standard impulse waveshapes, test generators*

1. INTRODUCTION

For the testing of equipment in high-voltage technique the generators have to produce the defined waveshapes as given in the relevant standards, and the testing waveshapes have to be repeatable within tolerances which are also given in these standards. Frequency analysis of such waveshapes is important for the study of their effects on the tested equipment. It is also important for the choice and use of measuring instruments and their characteristics in frequency domain (their frequency response and bandwidth). Such analysis is significant for the design of test generators [1].

Fourier transform (FT) of aperiodic signals results in continuous spectra over frequency domain, whereas periodic signals have discrete spectra and their amplitudes at each frequency

Received June 13, 2022; revised July 22, 2022 accepted August 08, 2022

Corresponding author: Vesna Javor

Department of Power Engineering, Faculty of Electronic Engineering, University of Niš

E-mail: vesna.javor@elfak.ni.ac.rs

represent the strength of the signal at that frequency. However, impulse voltages and currents testing signals are also called energy signals as they have finite energy in time domain. They are characterized by energy spectral density which is proportional to the square of the signal integrated over the time domain. According to the Parseval's relation, the same value is obtained if the square of its Fourier transform amplitude is integrated over the frequency domain [2].

If an impulse function is approximated by e.g. double-exponential function (DEXP) [3]-[4], it may be further replaced by the terms of Multi-peaked analytically extended function (MP-AEF) [5], and its Fourier transform may be obtained analytically by using Piecewise Fourier Transform (PWFT) [6]. There are various applications of exponential functions for approximation of waveshapes and it is proved in this paper that MP-AEF may be used equally without introducing any error.

The sequence in which the analysis is carried out is the following:

- the parameters of DEXP are obtained so to approximate the impulse waveshape by using Least squares method (LSQM) [3]-[4], or by using Marquardt method for least squares estimation of nonlinear MP-AEF parameters (MLSM) [7];
- frequency spectrum is determined analytically by using PWFT [6] applied to the MP-AEF terms;
- frequency bandwidth of the signal is determined so to use these results for further calculations or for the choice of measuring instruments, and possible peaks in the amplitude spectrum are analyzed so to check the periodicity of the waveshape (if it has dumped oscillations).

This procedure is applicable to impulse functions with multiple and sharp peaks which can be well approximated by the terms of MP-AEF. Some typical impulse waveshapes, such as 1.2/50 $\mu\text{s}/\mu\text{s}$, 10/350 $\mu\text{s}/\mu\text{s}$, 10/700 $\mu\text{s}/\mu\text{s}$, 10/1000 $\mu\text{s}/\mu\text{s}$, and 250/2500 $\mu\text{s}/\mu\text{s}$, are analyzed in this paper. The frequencies at which Fourier transforms amplitudes of these signals decay to a certain percentage of the amplitude at the frequency $f=0$ are also given in this paper. This is important for the analysis of induced effects on the equipment under test and for any further calculations in the frequency domain.

Other waveshapes can be analyzed by the presented procedure, including 8/20 $\mu\text{s}/\mu\text{s}$ waveshape [8] and oscillatory dumped waveshapes of test generators, as they are suitable for approximation by the terms of MP-AEF, but not suitable for approximation by DEXP. To confirm the procedure on such functions, the results are given in this paper for the Fourier transform of the Sinc function approximated by a few terms of MP-AEF.

2. TYPICAL IMPULSE VOLTAGES AND CURRENTS OF THE TEST GENERATORS

Impulse waveshapes are usually defined by several parameters, such as the peak value U_m for the voltage or I_m for the current at the instant t_m , and the two time parameters T_1 and T_2 . T_1 is the front time which is the time interval between the instant t_a at the point A when the signal is either 30% (Fig. 1) or 10% of the peak value and the instant t_b at the point B when the signal is 90% of the peak value.

T_2 is the time interval between the instant t_a' when the signal starts at the virtual origin O_1 and the instant t_k when the signal is half of the peak value (Fig. 2). P_1 is the saddle point at t_1 in the rising part (Fig. 1), P_2 the saddle point at t_2 in the decaying part (Fig. 2).

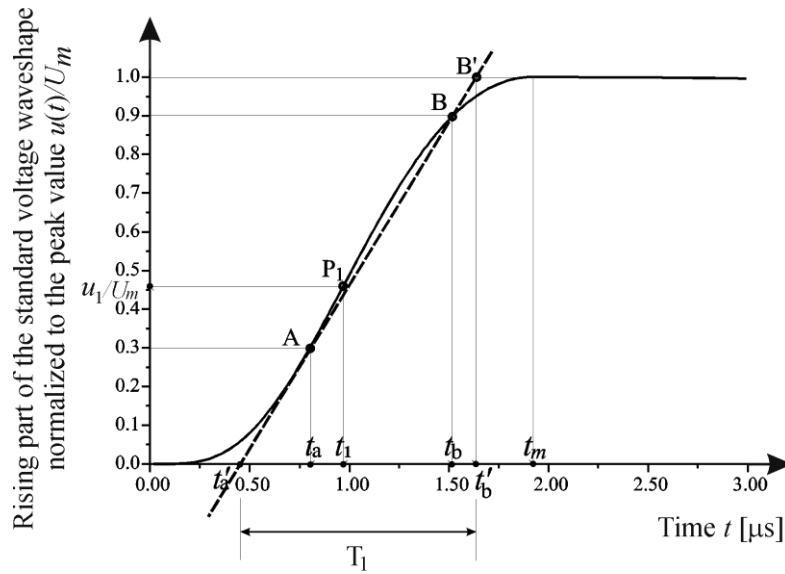


Fig. 1 Rising part of the voltage 1.2/50 $\mu\text{s}/\mu\text{s}$ normalized to the peak value versus time t

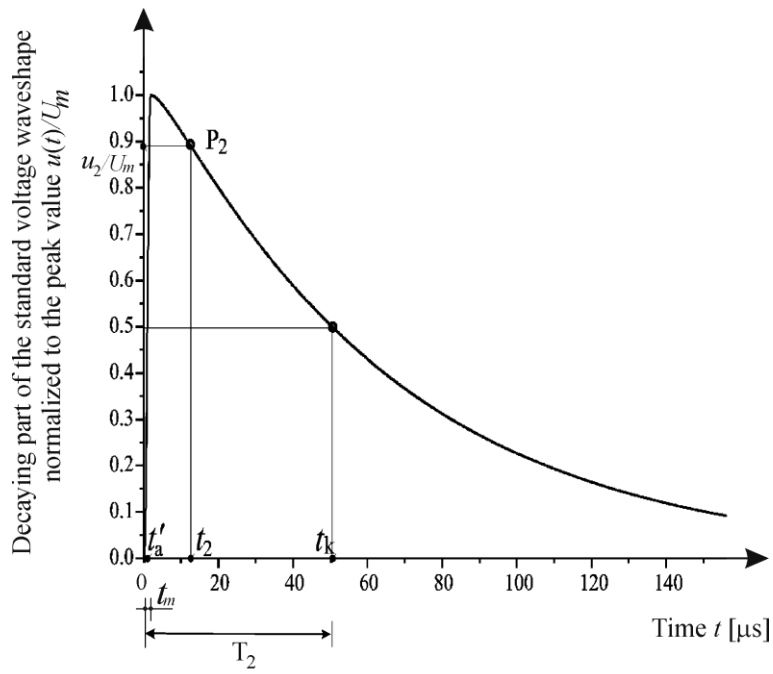


Fig. 2 Decaying part of the voltage 1.2/50 $\mu\text{s}/\mu\text{s}$ normalized to the peak value $u(t)/Um$ versus time t

The IEC 60060-1:2010 Standard [9] gives general definitions and test requirements for the high-voltage test techniques. The standard voltage testing waveshape in high-voltage engineering is defined by $T_1/T_2 = 1.2/50 \mu\text{s}/\mu\text{s}$, as given in Figs. 1 and 2. If approximated by DEXP function, the parameters of some typical waveshapes are calculated using least squares method for parameters estimation in [3], as given in Table 1, and in [4] for the switching impulse 250/2500 $\mu\text{s}/\mu\text{s}$ approximated by DEXP.

Table 1 DEXP parameters obtained by using the least squares method [3], [4]

Waveshapes T_1/T_2	η	α (s^{-1})	β (s^{-1})
1.2/50 $\mu\text{s}/\mu\text{s}$	0.95847	14732.18	2080312.7
10/350 $\mu\text{s}/\mu\text{s}$	0.9511	2121.76	245303.6
10/700 $\mu\text{s}/\mu\text{s}$	0.97423	1028.39	257923.7
10/1000 $\mu\text{s}/\mu\text{s}$	0.98135	712.41	262026.6
250/2500 $\mu\text{s}/\mu\text{s}$	0.9057971	316.95721	16003.329

DEXP function approximating impulse voltage is given by

$$u(t) = U_m (e^{-\alpha t} - e^{-\beta t}) = \frac{U}{\eta} (e^{-\alpha t} - e^{-\beta t}) \quad (1)$$

for U the voltage value that multiplied by the peak correction factor η results in the peak voltage value U_m , whereas α and β are the parameters of the DEXP function.

The peak correction factor is the function of α and β ,

$$\eta = e^{-\alpha t_m} - e^{-\beta t_m} \quad (2)$$

for t_m the time instant of the maximum value U_m and

$$t_m = \frac{1}{\beta - \alpha} \ln \frac{\beta}{\alpha} \quad (3)$$

The waveshape 10/350 $\mu\text{s}/\mu\text{s}$ is the lightning current waveshape of the first positive stroke as given in the standard IEC 62305 [10]. This function is very important because the positive first stroke has the highest specific energy among lightning discharge types. Other impulse lightning discharge currents, such as 0.25/100 $\mu\text{s}/\mu\text{s}$ for the subsequent negative stroke and 1/200 $\mu\text{s}/\mu\text{s}$ for the first negative stroke, are not typical for test generators, but they are used for the analysis of induced voltages in electric power systems due to short rising times.

The waveshapes of electrostatic discharge (ESD) generators are given in [11], and important characteristics of impulse generators are listed in [12].

A simplified scheme of the circuit to produce an ESD impulse for the testing of devices is given in Fig. 3, for C_d the distributed capacitance which exists between the generator and its surroundings, $C_d + C_s$ of the typical value of 150 pF, R_d of the typical value of 330 Ω , R_c of the typical value between 50 M Ω and 100 M Ω , as given in [9].

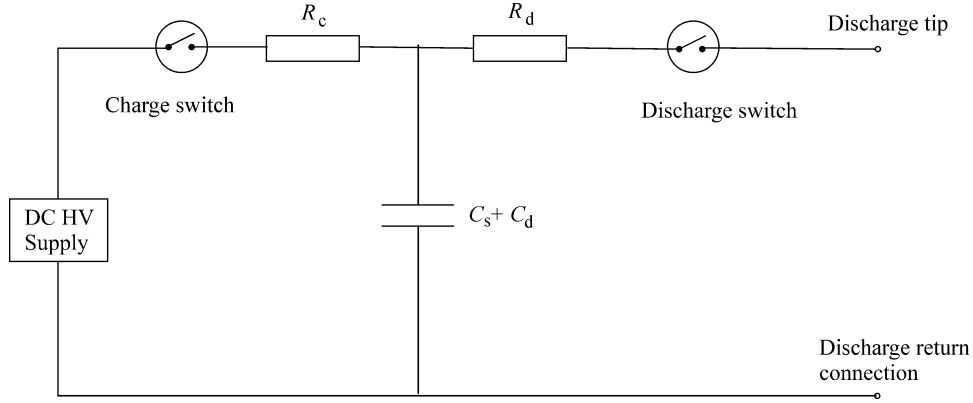


Fig. 3 Simplified scheme of the circuit to produce ESD impulse for testing according to [9]

Experimental set ups and realization of impulse generators are discussed in [13]-[15]. Various realizations of impulse generators for testing in high voltage engineering are given in [16]-[18]. Real time conditions are the reason of defining intervals for typical parameters of the waveshapes in relevant standards, so that repeatability of testing and experiments can be achieved and compliance proved with the standardized values.

3. NUMERICAL EXAMPLES

3.1. Multi-peaked analytically extended function (MP-AEF) and its Fourier transform

The MP-AEF function [5] term is given by

$$\begin{aligned}
 x(t) &= C_1 + (C_2 - C_1) \left[\frac{t - t_b}{t_e - t_b} \exp \left(1 - \frac{t - t_b}{t_e - t_b} \right) \right]^a = \\
 &C_1 + (C_2 - C_1) \left[\left(\frac{1}{t_e - t_b} t - \frac{t_b}{t_e - t_b} \right) \exp \left(- \frac{t}{t_e - t_b} + \frac{t_e}{t_e - t_b} \right) \right]^a = \\
 &C_1 + (C_2 - C_1) [(D_1 t + D_2) \exp(1 - D_1 t - D_2)]^a
 \end{aligned} \tag{4}$$

for the parameter a and coefficients C_1 , C_2 , $D_1 = (t_e - t_b)^{-1}$ and $D_2 = -t_b (t_e - t_b)^{-1} = -t_b D_1$. C_1 is the function value at the beginning t_b of using approximation term, so that $y(t_b) = C_1$, and C_2 is the function value at the end t_e of using approximation term, so that $y(t_e) = C_2$.

The DEXP function (1) may be replaced by four terms (4) using transformation

$$\begin{aligned}
 x(t) &= X_m [\exp(-\alpha t) - \exp(-\beta t)] = \\
 &X_m [(\alpha + 1) \exp(-\alpha t) - \alpha t \exp(-1) \exp(1 - \alpha t) \\
 &\quad - (\beta + 1) \exp(-\beta t) + \beta t \exp(-1) \exp(1 - \beta t)]
 \end{aligned} \tag{5}$$

Fourier transform of each term (4) is obtained analytically, for $C_1 \neq 0$, as

$$Y(p) = \frac{C_1}{p} + \frac{(C_2 - C_1) \exp(a + D_2 p / D_1)}{D_1 (a + p / D_1)^{a+1}} \gamma[a+1, z_1, z_2] \quad (6)$$

for the Gamma function defined by

$$\gamma[a+1, z_1, z_2] = \int_{z_1}^{z_2} t^a \exp(-t) dt \quad (7)$$

with the arguments $a+1$, $z_1 = (D_1 t_1 + D_2)(a + p / D_1)$, and $z_2 = (D_1 t_2 + D_2)(a + p / D_1)$.

3.2. Fourier transform of the impulse voltage 1.2/50 $\mu\text{s}/\mu\text{s}$ waveshape

The approximation of any impulse function with one peak may be also done by just two MP-AEF terms, so that the impulse voltage 1.2/50 $\mu\text{s}/\mu\text{s}$ may be approximated by

$$u(t) = \begin{cases} u_1(t) = U_m \left[\frac{t}{t_m} \exp\left(1 - \frac{t}{t_m}\right) \right]^a, & 0 \leq t < t_m \\ u_2(t) = U_m \left[\frac{t}{t_m} \exp\left(1 - \frac{t}{t_m}\right) \right]^b, & t_m \leq t \end{cases} \quad (8)$$

for a and b the parameters of the two MP-AEF terms $u_1(t)$ and $u_2(t)$, respectively. The first term is the same as (4) for $C_1=0$, $C_2=U_m$, $t_e = t_m$, $t_b = 0$, $D_1 = t_m^{-1}$ and $D_2 = 0$. This results in the piece-wise function (6) for $t_m = 1.9 \mu\text{s}$ of the peak value and parameters $a=4$ and $b=0.03126$. Rising part of the function $u_1(t)$ represents the rising part of $u(t)$ and is given by blue line in Fig. 4. Decaying part of $u_2(t)$ represents the decaying part of $u(t)$ and is given by red line in Fig. 4.

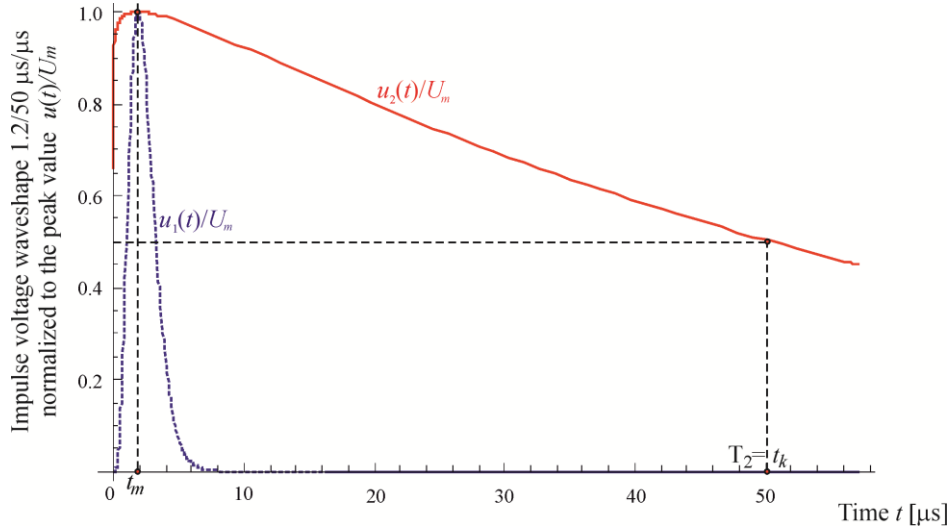


Fig. 4 Impulse voltage waveshape 1.2/50 $\mu\text{s}/\mu\text{s}$ normalized to the peak value versus time t , approximated by the two MP-AEF terms $u_1(t)/U_m$ (blue line) and $u_2(t)/U_m$ (red line).

The result for the Fourier transform of the function $1.2/50 \mu\text{s}/\mu\text{s}$ is given in Fig. 5. It can be noticed that the amplitude of the Fourier transform of that waveshape is approximately constant up to the frequency of 1kHz. At the frequency $f_1 \cong 4\text{kHz}$ the amplitude is approximately half of the value at low frequencies. At the frequency $f_2 \cong 200\text{kHz}$ the amplitude is approximately 1% of the value at low frequencies.

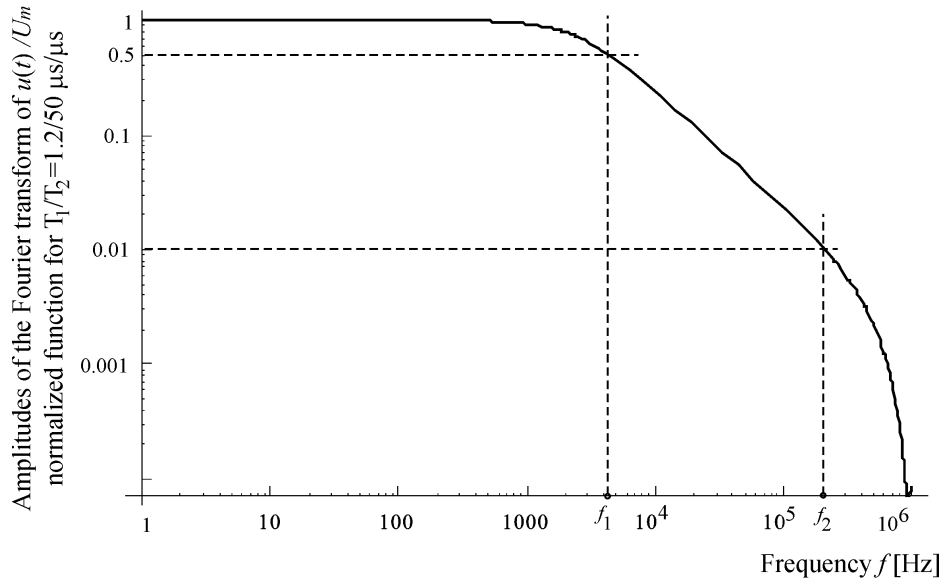


Fig. 5 Amplitudes of the Fourier transform of the impulse $1.2/50 \mu\text{s}/\mu\text{s}$ versus frequency f .

3.3. Fourier transforms of $10/350 \mu\text{s}/\mu\text{s}$, $10/700 \mu\text{s}/\mu\text{s}$ and $10/1000 \mu\text{s}/\mu\text{s}$ waveshapes

Standard lightning current impulse $i(t)/I_m$ of the first positive stroke is defined by $10/350 \mu\text{s}/\mu\text{s}$ and approximated by MP-AEF terms. Its Fourier transform is presented in Fig. 6. The amplitudes of the Fourier transform are approximately constant up to the frequency of 100Hz. At $f_1 \cong 200\text{Hz}$ the amplitude is approximately half of the value at low frequencies, whereas at $f_2 \cong 10\text{kHz}$ the amplitude is approximately 1% of the value at low frequencies.

Fourier transforms of the three typical impulse waveshapes are presented in Fig. 7 and denoted by a) $10/350 \mu\text{s}/\mu\text{s}$, b) $10/700 \mu\text{s}/\mu\text{s}$, and c) $10/1000 \mu\text{s}/\mu\text{s}$. These results show that the amplitudes of the Fourier transforms are approximately constant up to the frequency of 100Hz for all the three waveshapes. At $f_{1a} \cong 200\text{Hz}$, $f_{1b} \cong 300\text{Hz}$ and $f_{1c} \cong 600\text{Hz}$ the amplitudes are approximately half of the value at low frequencies, whereas at $f_{2a} \cong 10\text{kHz}$, $f_{2b} \cong 15\text{kHz}$ and $f_{2c} \cong 25\text{kHz}$ the amplitude is approximately 1% of the value at low frequencies.

Impulse $10/700 \mu\text{s}/\mu\text{s}$ presents an open-circuit voltage waveshape, whereas $10/1000 \mu\text{s}/\mu\text{s}$ may present either open-circuit voltage waveshape or short-circuit current waveshape of the impulse generator, but in this paper all the three waveshapes were analyzed together in Fig. 7, so to notice the influence of the decaying time on the frequency spectrum of the waveshape.

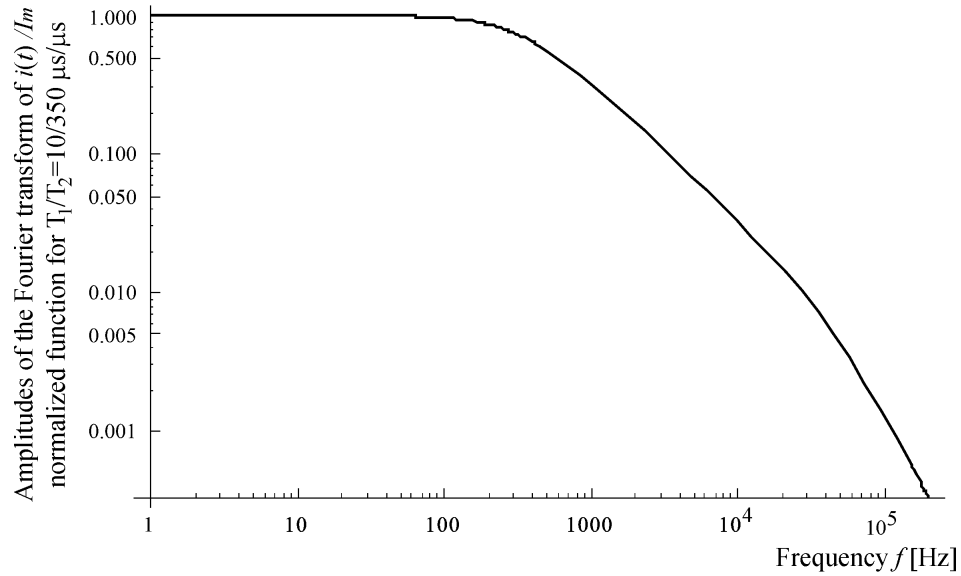


Fig. 6 Amplitudes of the Fourier transform of the impulse $10/350 \mu\text{s}/\mu\text{s}$ versus frequency f

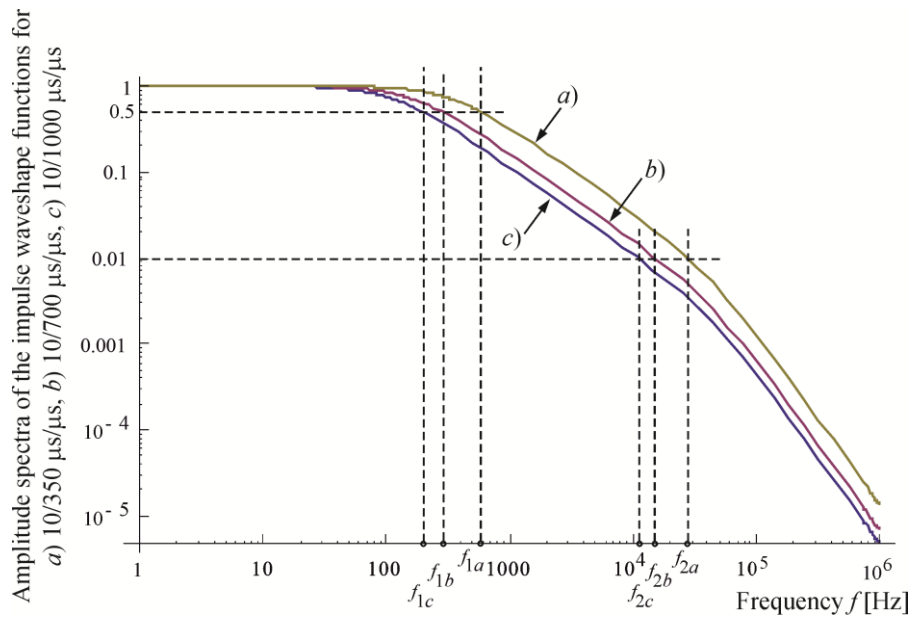


Fig. 7 Amplitude spectra of the impulse waveshapes: *a*) $10/350 \mu\text{s}/\mu\text{s}$, *b*) $10/700 \mu\text{s}/\mu\text{s}$, *c*) $10/1000 \mu\text{s}/\mu\text{s}$ versus frequency f

Results presented in Figs. 5, 6 and 7 may be used to estimate the frequency bandwidth of the measuring instruments used in testing of the equipment according to the desired accuracy and relevant standards. For the computation of the induced effects of such signals in frequency domain is enough to take into account frequencies up to 1MHz.

3.4. Fourier transform of the switching voltage 250/2500 μs/μs waveshape

Switching impulse waveshapes are slower in the rising part than the lightning impulse waveshapes, and have longer time duration in total. For the impulse $T_1/T_2 = 250/2500$ μs/μs the Fourier transform is given in Fig. 8. The amplitude of the Fourier transform is approximately constant up to the frequency of 10Hz. At $f_1 \cong 90$ Hz the amplitude is approximately half of the value at low frequencies, whereas at $f_2 \cong 3$ kHz the amplitude is about 1% of the value at low frequencies.

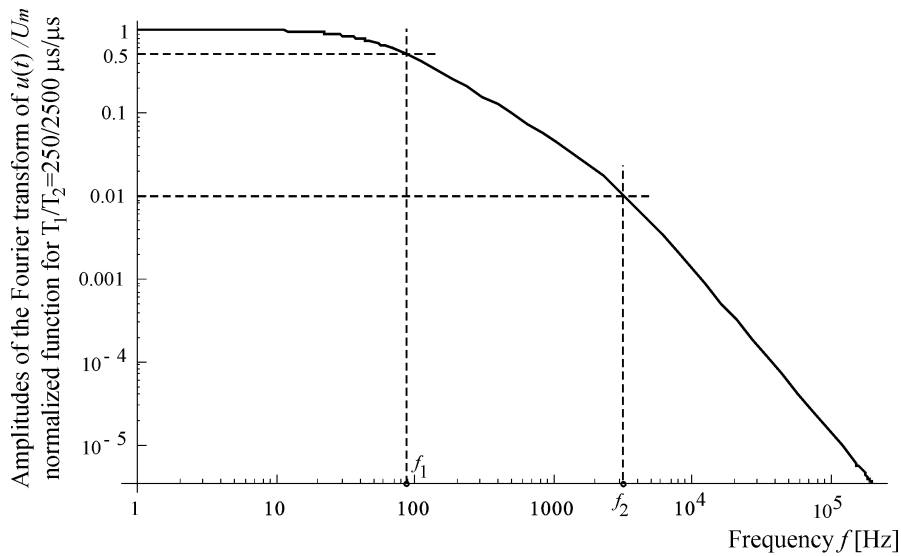


Fig. 8 Amplitudes of the Fourier transform of the switching impulse 250/2500 μs/μs versus frequency f

3.5. Fourier transform of the damped oscillations waveshapes

Standard 61000-4-12 impulse current, also denoted as ring wave, is given in Fig. 9. $Pk1$ denotes the first peak, $Pk2$ the second, $Pk3$ the third, and $Pk4$ the fourth. Only $Pk1$ is specified for the current waveform. T_1 is the rise time and T the period of oscillations.

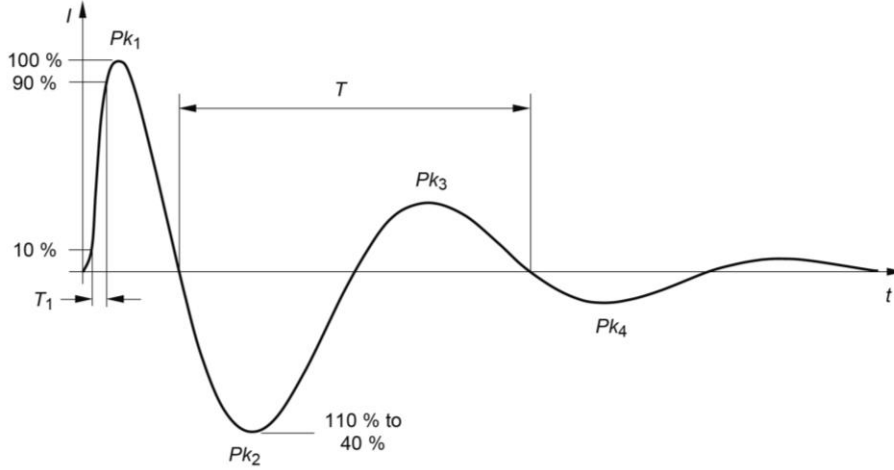


Fig. 9 Standard 61000-4-12 [8] impulse current waveshape

Generation of 8/20 $\mu\text{s}/\mu\text{s}$ impulse current assumes damped oscillations with the rise time $T_1 = 8 \mu\text{s} \pm 20\%$ and the decaying time $T_2 = 20 \mu\text{s} \pm 20\%$ for the first peak Pk_1 . The advantage of MP-AEF over DEXP is that it is suitable to approximate waveshapes with multiple peaks as given in Fig. 9.

Sinc function is also an example of the damped oscillations waveshapes. Normalized Sinc function is defined, for $t \neq 0$, as

$$\text{Sinc}(t) = \frac{\text{Sin}(\pi t)}{\pi t} \quad (9)$$

This function is presented in Fig. 10, for $t \in (0, 6\text{s}]$.

It is approximated by six terms of MP-AEF given by (4), but for $D_{1i} = t_{mi}^{-1}$ and $D_{2i} = t_{mi}^{-1} \sum_{k=0}^{i-1} t_{mk}$, so that the terms are given by

$$x_i(t) = C_{1i} + (C_{2i} - C_{1i}) \left[\left(\frac{t - \sum_{k=0}^{i-1} t_{mk}}{t_{mi}} \right) \exp \left(1 - \frac{t - \sum_{k=0}^{i-1} t_{mk}}{t_{mi}} \right) \right]^a \quad (10)$$

for $t_{m0} = 0$. Parameter $a=3$ for all the terms and other parameters are given in Table 2.

The complete procedure for obtaining function parameters is presented in [19].

Amplitude spectrum i.e. modulus of the Fourier transform of this function is presented in Fig. 11 for $f \in [0.01\text{Hz}, 10\text{MHz}]$, and in Fig. 12 for $f \in [0.1\text{Hz}, 1\text{Hz}]$, so to notice the peak at $f = 0.5\text{Hz}$ due to $T=2\text{s}$ (Fig. 10).

For the damped oscillations of the impulse current waveshape 8/20 $\mu\text{s}/\mu\text{s}$ with the period about $T=330\mu\text{s}$, the peak in its Fourier transform appears at about $f = 3\text{kHz}$.

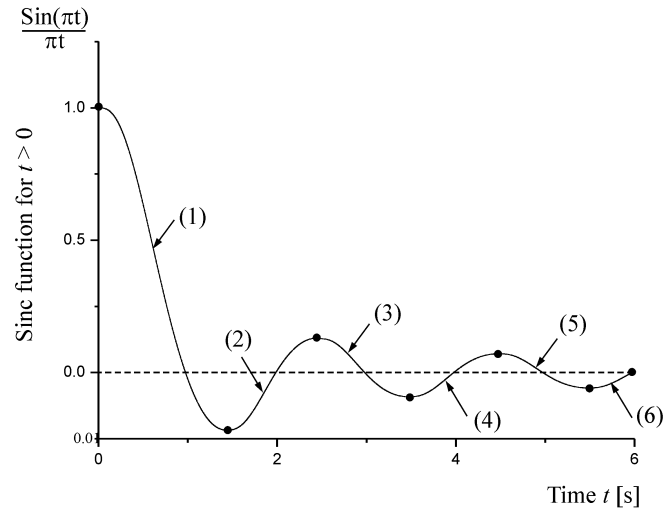


Fig. 10 Sinc function approximated by six MP-AEF terms, for $t \in (0, 6\text{ s}]$

Table 2 Parameters of the six MP-AEF terms

Term i	C_{1i}	C_{2i}	t_{mi}
1	1	- 0.21722	1.431
2	- 0.21722	0.12837	1.028
3	0.12837	-0.0913	1.012
4	-0.0913	0.07091	1.006
5	0.07091	-0.05797	1.004
6	-0.05797	0.04903	1.003

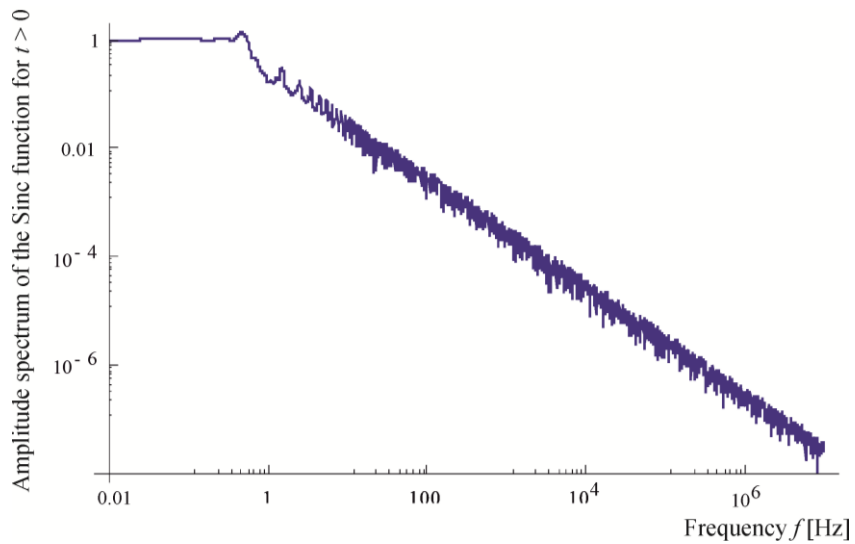


Fig. 10 Amplitude spectrum of the function from Fig. 9 versus frequency $f \in [0.01\text{Hz}, 10\text{MHz}]$

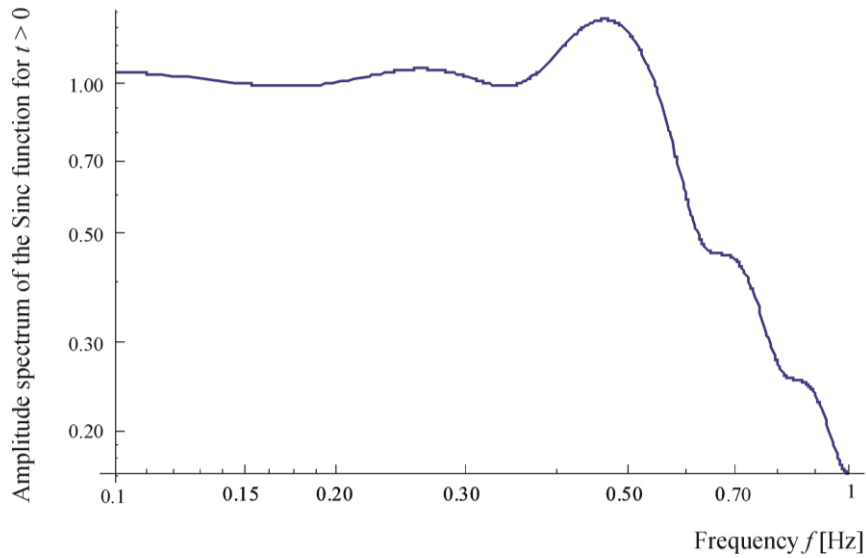


Fig. 11 Amplitude spectrum of the function from Fig. 9 versus frequency $f \in [0.1\text{Hz}, 1\text{Hz}]$

4. CONCLUSION

Electrostatic discharge currents and also lightning discharge currents are of impulse waveshapes. Induced voltages and currents in electric circuits due to fast changing external electromagnetic fields are of impulse waveshapes. Fast transients in electric circuits due to switching operations are of impulse waveshapes. Due to all these, the testing generators have to produce such waveshapes [20]-[22] in order to check the equipment according to the standards.

Fourier transforms of typical impulse waveshapes of test generators in high-voltage technique are obtained by using terms of MP-AEF. The procedure is suitable for aperiodic functions because Fourier transform of MP-AEF terms is obtained analytically by using Gamma functions.

Frequency analysis of the waveshapes $1.2/50 \mu\text{s}/\mu\text{s}$, $10/350 \mu\text{s}/\mu\text{s}$, $10/700 \mu\text{s}/\mu\text{s}$, $10/1000 \mu\text{s}/\mu\text{s}$, and $250/2500 \mu\text{s}/\mu\text{s}$, shows the necessary bandwidths for frequency domain calculations and also for measurements. The comparison of the three functions with the same rising time $10/350 \mu\text{s}/\mu\text{s}$, $10/700 \mu\text{s}/\mu\text{s}$, and $10/1000 \mu\text{s}/\mu\text{s}$ is also given in this paper. The procedure is also applied to the oscillatory damped function in this paper as such waveshapes are important for testing of the equipment in high-voltage technique.

In the future research, other oscillatory damped functions as $8/20 \mu\text{s}/\mu\text{s}$, $4/16 \mu\text{s}/\mu\text{s}$ and $5/320 \mu\text{s}/\mu\text{s}$ will be analyzed by using terms of MP-AEF to approximate the waveshapes, and afterwards PWFT is going to be used to obtain their frequency spectra.

Acknowledgement: *The paper is a part of the research done within the project no. 451-03-68/2022-14 of the Faculty of Electronic Engineering in Niš, supported by the Ministry of Education, Science and Technological Development of the Republic of Serbia.*

REFERENCES

- [1] I. F. Gonos, N. Leontides, F. V. Topalis, I. A. Stathopoulos, "Analysis and design of an impulse current generator", *WSEAS Transactions on Circuits and Systems*, vol. 1, pp. 38-43, January 2002.
- [2] K. L. Kaiser, *Electromagnetic Compatibility Handbook*, CRC Press, 2015, Chapter 12, pp. 165.
- [3] D. Lovrić, S. Vujević, T. Modrić, "Least squares estimation of double-exponential function parameters," In Proceedings of the 11th Int. Conf. IIEC 2013, Niš, Serbia, Sept. 2013, pp. 1-4.
- [4] K. Schon, High impulse voltage and current measurement techniques, Springer, 2013, Chapter 2, pp. 5-9.
- [5] V. Javor, "Multi-peaked functions for representation of lightning channel-base currents", In Proceedings of the ICLP 31st Int. Conference on Lightning Protection ICLP 2012, Sep. 2-7, 2012, OVE Vienna, Austria, Sep. 2012.
- [6] V. Javor, "Piece-wise Fourier transform of aperiodic functions," In Proceedings of the 21st Int. Symp. INFOTEH-JAHORINA 2022, March 2022, pp. 1-4.
- [7] K. Lundengård, M. Rančić, V. Javor, S. Silvestrov, "Estimation of parameters for the multi-peaked AEF current functions", In Proceedings of the 16th Applied Stochastic Models and Data Analysis International Conference (ASMDA) and 4th Demographics Workshop, Piraeus, Greece, 30 June - 4 July 2015, pp. 623-636.
- [8] IEC 61000-4-12 standard, Electromagnetic compatibility (EMC) – Part 4-12: Testing and measurement techniques – Ring wave immunity test, Ed. 3.0, 2017, <https://webstore.iec.ch/publication/29872>
- [9] IEC 60060-1:2010 standard, High voltage test techniques - Part 1: General definitions and test requirements, Ed. 3.0, 2010, <https://webstore.iec.ch/publication/300>
- [10] IEC 62305-1 standard, Protection against lightning - Part 1: General principles, Ed. 2.0, 2010-2012.
- [11] EMC – Part 4-2: Testing and Measurement Techniques – Electrostatic Discharge Immunity Test, IEC Int. Standard 61000-4-2, Ed. 2, 2008-2012.
- [12] http://pes-spdc.org/sites/default/files/Impulse_generatorsaddedrev3.pdf
- [13] Z. Javid, K.-J. Li, K. Sun, and A. Unbree, "Cost Effective Design of High Voltage Impulse Generator and Modeling in MATLAB", *J. Electr. Eng. Technol.*, vol. 13, no. 3, pp. 1346-1354, 2018.
- [14] V. C. Vita, G. P. Fotis, and L. Ekonomou "Parameters' optimization methods for the electrostatic discharge current equation", *Int. Journal of Energy*, vol. 11, pp. 1-6, 2017.
- [15] G. P. Fotis, F. E. Asimakopoulou, I. F. Gonos, and I. A. Stathopoulos, "Applying genetic algorithms for the determination of the parameters of the electrostatic discharge current equation", *Meas. Sci. Technol.*, vol. 17, pp. 2819–2827, 2006.
- [16] M. Abdel-Salam, High-voltage engineering: theory and practice, rev. and expanded. CRC Press, 2018.
- [17] E. Kuffel, W. S. Zaengl, J. Kuffel, *High voltage engineering: fundamentals*, Newnes, 2000, pp. 48-74.
- [18] S. Mehta, P. Basak, K. Anelis, A. Paramane, "Simulation of single and multistage impulse voltage generator using Matlab Simulink", In Proceedings of the 2018 International Conference on Computing, Power and Communication Technologies (GUCON), IEEE, 2018, pp. 641-646.
- [19] K. Lundengård, M. Rančić, V. Javor, S. Silvestrov, "Electrostatic discharge currents representation using the analytically extended function with p peaks by interpolation on a D-optimal design", *Facta Universitatis, Series Electronics and Energetics*, vol. 32, no. 1, pp. 25-49, 2019.
- [20] Y. Trotsenko, V. Brzhezitsky, O. Protsenko, Y. Haran, "Simulation of Impulse Current Generator for Testing Surge Arresters Using Frequency Dependent Models", *Technology audit and production reserves*, vol. 1, no. 1 (57), pp. 25-29, 2021.
- [21] K. Filik, G. Karnas, G. Masłowski, M. Oleksy, R. Oliwa, K. Bulanda, "Testing of Conductive Carbon Fiber Reinforced Polymer Composites Using Current Impulses Simulating Lightning Effects", *Energies*, vol. 14, no. 7899, 2021.
- [22] P. Ghosh, B. Chakraborty, S. Dalai, S. Chatterjee, "Simulation and Real-Time Generation of Non-Standard Lightning Impulse Voltage Waveforms", In Proceedings of the 2022 IEEE Int. Conf. on Distributed Computing and Electrical Circuits and Electronics (ICDCECE), 2022, pp. 1-5.